Geologica Acta, Vol.7, Nº 4, December 2009, 413-429
DOI: 10.1344/104.000001447
Available online at www.geologica-acta.com
geologica acta

Metamorphism on Chromite Ores from the Dobromirtsi Ultramafic Massif, Rhodope Mountains (SE Bulgaria)

J.M. GONZÁLEZ-JIMÉNEZ [1] T. KERESTEDJIAN [2] J.A. PROENZA [3] and F. GERVILLA [1]

[1] Departamento de Mineralogía y Petrología and Instituto Andaluz de Ciencias de la Tierra (Universidad de Granada-CSIC), Facultad de Ciencias
Avda. Fuentenueva s/n, 18002 Granada, Spain. González-Jiménez E-mail: jmgonzj@ugr.es, Gervilla E-mail: gervilla@ugr.es

[2] Geological Institute, Bulgarian Academy of Sciences
24 Georgi Bonchev Str., 1113 Sofia, Bulgaria. E-mail: thomas.kerestedjian@gmail.com

[3] Departament de Cristal·lografia, Mineralogia i Dipòsits Minerals, Facultat de Geologia, Universitat de Barcelona
Martí i Franquès s/n, 08028 Barcelona, Spain. E-mail: japroenza@ub.edu

ABSTRACT

Podiform chromitite bodies occur in highly serpentinized peridotites at Dobromirtsi Ultramafic Massif (Rhodope Mountains, southeastern Bulgaria). The ultramafic body is believed to represent a fragment of Palaeozoic ophiolite mantle. The ophiolite sequence is associated with greenschist - lower-temperature amphibolite facies metamorphosed rocks (biotitic gneisses hosting amphibolite). This association suggests that peridotites, chromitites and metamorphic rocks underwent a common metamorphic evolution. Chromitites at Dobromirtsi have been strongly altered. Their degree of alteration depends on the chromite/silicate ratio and to a lesser extent, on the size of chromitite bodies. Alteration is recorded in individual chromite grains in the form of optical and chemical zoning. Core to rim chemical trends are expressed by MgO- and Al_2O_3- impoverishment, mainly compensated by FeO and/or Fe_2O_3 increases. Such chemical variations correspond with three main alteration events. The first one was associated with ocean-floor metamorphism and was characterized by a lizardite replacement of olivine and the absence of chromite alteration. The second event took place during greenchist facies metamorphism. During this event, MgO- and SiO_2-rich fluids (derived from low temperature serpentinization of olivine and pyroxenes) reacted with chromite to form chlorite; as a consequence, chromite became altered to a FeO- and Cr_2O_3-rich, Al_2O_3-poor chromite. The third event, mainly developed during lower temperature amphibolite facies metamorphism, caused the replacement of the primary and previously altered chromite by Fe_2O_3-rich chromite (ferritchromite).

KEYWORDS | Ophiolite. Chromite. Metamorphism. Dobromirtsi Ultramafic Massif. Bulgaria.

INTRODUCTION

Cr-spinel [(Mg, Fe^{2+}) (Cr, Al, Fe^{3+})$_2O_4$] is a common accessory mineral in ultramafic and mafic rocks. It also forms monomineralic bodies of economic value which are found scattered in the mantle section of ophiolite complexes worldwide. In such settings, Cr-spinel displayes a large range of composition, reflecting their primary, magmatic origin. Because Cr-spinel chemistry is sensitive to unaltered melt composition, its primary composition is used as a petrogenetic indicator (Irvine, 1967; Hil and Roeder, 1974; Maurel and Maurel, 1982; Dick and Bullen, 1984; Roeder and Reynolds, 1991; Arai, 1992; Stowe, 1994; Zhou and Robinson, 1997; Zhou et al., 1998; Proenza et al., 1999; Barnes and Roeder, 2001). Chemical modifications related to subsolidus equilibration during metamorphic or hydrothermal processes can significantly modify the primary composition of Cr-spinel. As a matter of fact, in serpentinized and metamorphosed rocks, the composition of Cr-spinel changes with alteration and metamorphic degree (Spangenberg, 1943; Thayer, 1966; Cerny, 1968; Beeson and Jackson, 1969; Ulmer, 1974; Evans and Frost, 1975; Bliss and McLean, 1975; Wylie et al., 1987; Thalhammer et al., 1990; Suita and Streider, 1996; Prichard et al., 2001; Proenza et al., 2004, 2008; Zaccarini et al., 2005; Garuti et al., 2007; among others), but the extent of chromite alteration still remains an open question.

In this paper, we examine the effects of serpentinization and metamorphism on the composition of Cr-spinel from a set of chromitite bodies, located in the Dobromirtsi Ultramafic Massif, southeastern Bulgaria, on the basis of their petrologic features and mineral chemistry. This massif is included in a metamorphosed area (central Rhodopes) which reached the amphibolite facies conditions. This fact, together with the low reactivity of Cr-spinel will allow the identification of different alteration/metamorphic events that affected these chromitite bodies. These events were recorded in Cr-spinel grains in the form of zoning patterns. The constraints provided here, on the origin of the different zoning patterns of Cr-spinel in relation to alteration/metamorphic reactions, are revealed to be an useful tool for studies that have chromite alteration mechanisms as their main targets.

GEOLOGICAL SETTING

The Rhodope Massif

The Rhodope Massif is a wide crystalline massif mainly composed of granitic and metamorphic rocks that extends along southeastern Bulgaria and northern Greece (Fig. 1). This massif represents a large orogen formed between the Srednogorie zone (underlain by European continental basement) and the present Aegean Sea (Marchev et al., 2005). Complex thrust tectonics and crustal thickening resulted from accretion of dominantly continental crustal material followed by polyphase regional metamorphism and final structuring by major low-angle extensional faults. Metamorphism is dominantly of amphibolite-facies with incipient migmatization in some areas and local relics of high to ultra-high pressure, eclogite facies metamorphism. Two major tectonostratigraphic complexes, the Gneiss-Migmatite Complex and the Variegated Complex, have been distinguished on the basis of dominant metamorphic rock composition. These units are separated, at least locally, by their degree of metamorphism and/or mappable low-angle detachment faults and thus they approximate the lower and upper plates of interpreted core complexes. The Gneiss-Migmatite Complex represents the tectonostratigraphically lower unit in extensional domes and in the studied area it builds the core of the Central Rhodopean Dome (Marchev et al., 2005). It is dominated by orthogneisses and is characterized by widespread evidence of incipient melting, with subordinate paragneisses, marbles and amphibolites located mainly in its upper parts. Ages reported for this complex suggest that it derived mainly from a Variscan or an older continental basement. The Variegated Complex is dominated by generally non-migmatized gneisses, amphibolites, scattered meta-ultramafic bodies and abundant marbles. In the studied area it makes up the upper plate of the Central Rhodopen Dome and is separated from its core complex by the Starsevo shear zone. The age of the initial rock formation and metamorphism is still discussed. Nevertheless, on the basis of SHRIMP dating of zircons in a gabbro that show neoproterozoic cores (570 Ma) overgrown by Variscan rims (300 to 350 Ma), some authors (Marchev et al., 2005) consider that these rocks and perhaps even their amphibolite-facies metamorphism are PreAlpine in age. These authors consider that amphibolite-facies metamorphism took place during a subduction process in Jurassic times.

According to Zhelyaskova-Panayotova and Economou-Eliopoulos (1994), there are dismembered metaophiolite bodies scattered within central and eastern Rhodope Massif. The ultramafic sequences of these ophiolite bodies are made up of highly deformed peridotites (harzburgites and dunites with minor amounts of lherzolites) and rocks of the cumulate sequence, including dunites, pyroxenite-dunites, olivine-pyroxenites, metagabbros and gabbropegmatites. Most of the ultramafic bodies are of small size and crop out in the eastern Rhodopes. Among them, the Dobromirtsi Ultramafic Massif is the biggest. This massif belongs to the Bojno

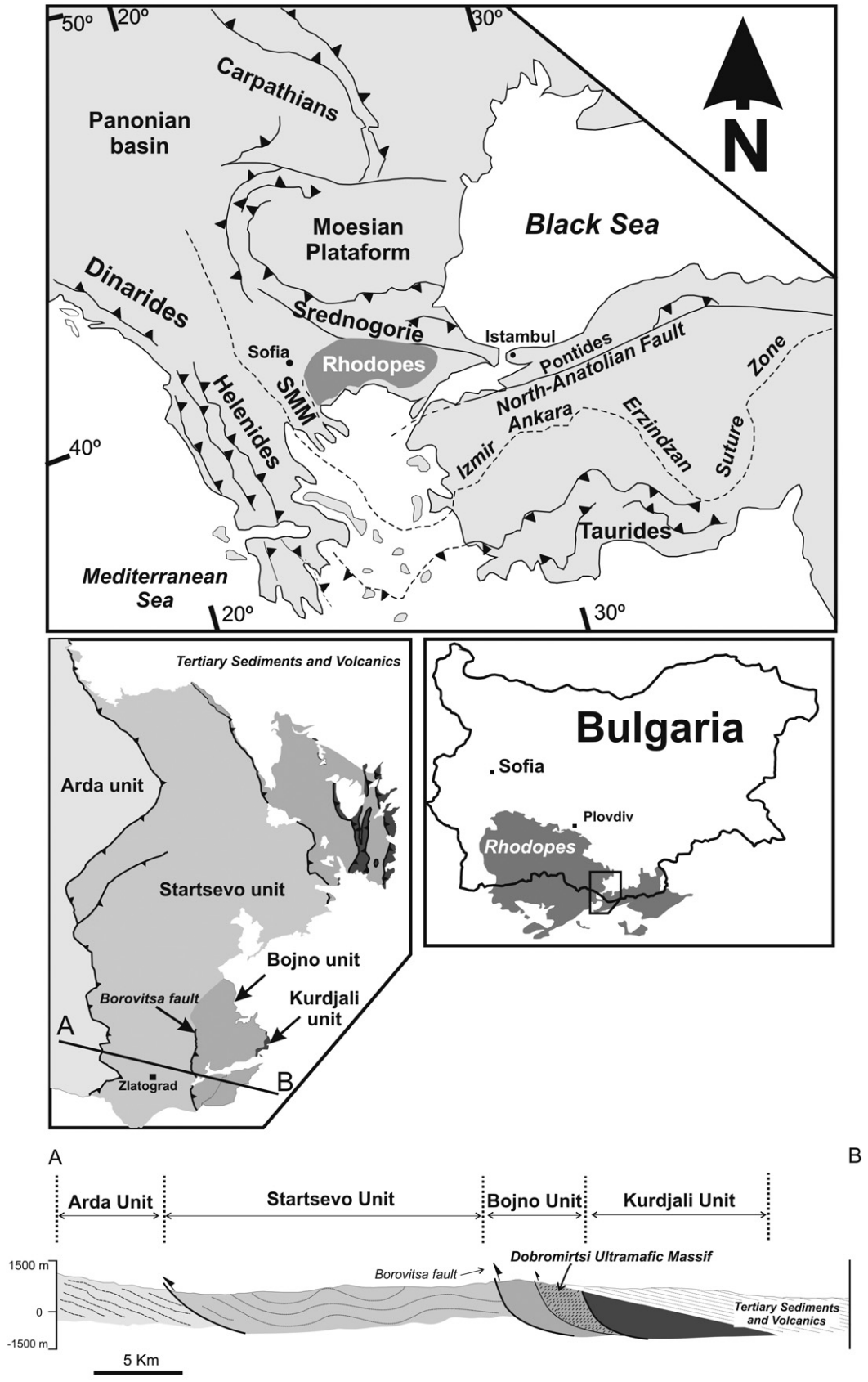

FIGURE 1 | **Location of the Rhodope Massif in the perimediterranean area, main lithotectonic units and simplified structural profile showing relationships between lithotectonic units (modified from Marchev et al., 2005).**

lithotectonic unit (the uppermost unit of the Variegated Complex) which is separated from the underlying Strartsevo unit by the Borovitsa fault zone (Fig. 1). The Bojno unit includes marbles, biotitic and fine-grained gneisses, porphyric and equigranular granites, massive metabasites, and highly serpentinized ultramafic rocks. The latter unit is thrusted by the Kurdjali unit and unconformably covered by tertiary sediments and volcanic rocks (Fig. 1).

The Dobromirtsi Ultramafic Massif

The Dobromirtsi Ultramafic Massif is a small ultramafic body (it crops out over 11 km^2) slightly elongated along the SW-NE direction (Fig. 2). The western part of the body thrusts over Palaeozoic metamorphic rocks (biotitic gneisses hosting amphibolites), whereas the eastern part is unconformably covered by continental sediments that host Oligocene volcanic rocks. The ultramafic rocks consist of highly serpentinized harzburgites, containing variable amounts of orthopyroxene, and dunites. Both types of rocks are cut by strongly folded (nearly isoclinal) veins of pyroxenites a few-centimetres thick. Mantle foliation (defined by the elongation of pyroxene and spinel crystals in porphyroclastic rocks) is obliterated by a late mylonitic foliation probably related either to the crustal emplacement of the peridotites or to the greenschist-amphibolite facies metamorphism that affected the central Rhodopes. This foliation strikes 20-60º, dipping 55-80º to the East, but is slightly parallel to vertical dipping near the western contacts of the body (Fig. 2). The dominant metamorphic alteration is serpentinization, but along tectonic faults the rocks were also affected by chloritization, carbonatization and talcization processes.

CHROMITE DEPOSITS

Chromitites at Dobromirtsi occur concordantly to the mylonitic foliation of the massif, and are located along a single dunite-rich horizon (Fig. 2). Locally, they are also cross-cut by pyroxenite veins.

Most chromitite bodies at Dobromirtsi were mined during the Second World War. However, accurate data about the mining history of the area and its ore production are unavailable. First scientific reports on these deposits were made by Payakov et al. (1961) and more recently by Zhelyaskova-Panayotova et al. (2000), who reported about two hundred small, podiform-like ore bodies in the massif. As a result of mining, only a few “in situ” chromitite bodies remain. Field data, along with the data reported by Payakov et al. (1961) and Zhelyaskova-Panayotova et al. (2000), suggest that chromite ore bodies form single, elongated lenses (tens of metres long, and less than 3 m thick) and layers (only a few metres long, and less than 0.5 m thick). Chromite is also concentrated in the form of small disseminations or veinlets, less than 5 cm thick.

SAMPLING AND ANALYTICAL METHODS

Eighty-two chromitite samples were collected from nine chromitite bodies (Fig. 2). Although, the majority of the collected chromitite samples come from blocks accumulated in dumps close to the old mining works, some samples were also collected in situ from the unexploited walls of various ore bodies. Polished thin sections of chromitites were studied by ore microscope, SEM, FESEM and ESEM prior to the quantitative, WDS analysis of the mineral phases by electron-microprobe. Analyses were obtained with a CAMECA SX50 electron microprobe at the *Serveis Cientificotècnics* of the *Universitat de Barcelona*. The analytical conditions were 20 kV accelerating voltage, 20 nA beam current, 2 μm beam diameter, and 10 s counting time. Calibration was performed using natural and synthetic standards: periclase (Mg), orthoclase (Al), diopside (Si), rutile (Ti), Cr_2O_3 (Cr), rhodonite (Mn), Fe_2O_3 (Fe), NiO (Ni) and sphalerite (Zn). Structural formulae of Cr-spinel were calculated assuming stoichiometry, following Carmichael’s (1967) procedure.

CHROMITITES

Petrography

Chromitite texture is mainly massive, but some bodies show semi-massive, disseminated, or locally nodular textures at their peripheral parts. Banded chromitites, with alternating chromite-rich and serpentine-rich layers are also present. Massive chromitites (>80% chromite) are composed of coarse aggregates of chromite crystals, up to 1.5 cm across. In contrast, semi-massive- and disseminated-textured ores (30-80% chromite) contain smaller (<1 cm), sometimes oriented chromite grains, and usually grade to more massive textures by increasing chromite content.

The degree of alteration of the different chromitite bodies is quite variable. It also varies within a single body. The degree of alteration depends on the size of the ore body and on the chromite/silicate ratio. Thus, massive chromitite from big ore bodies (D3, D4 and D8) are less altered than mid-sized and small ore bodies (D1, D2, D5, D6, D7 and D9). Likewise, chromite from disseminated chromitites displays higher degrees of alteration than chromite from semi-massive and massive chromitites. As a consequence, alteration increases from inner to outer parts of chromitite bodies.

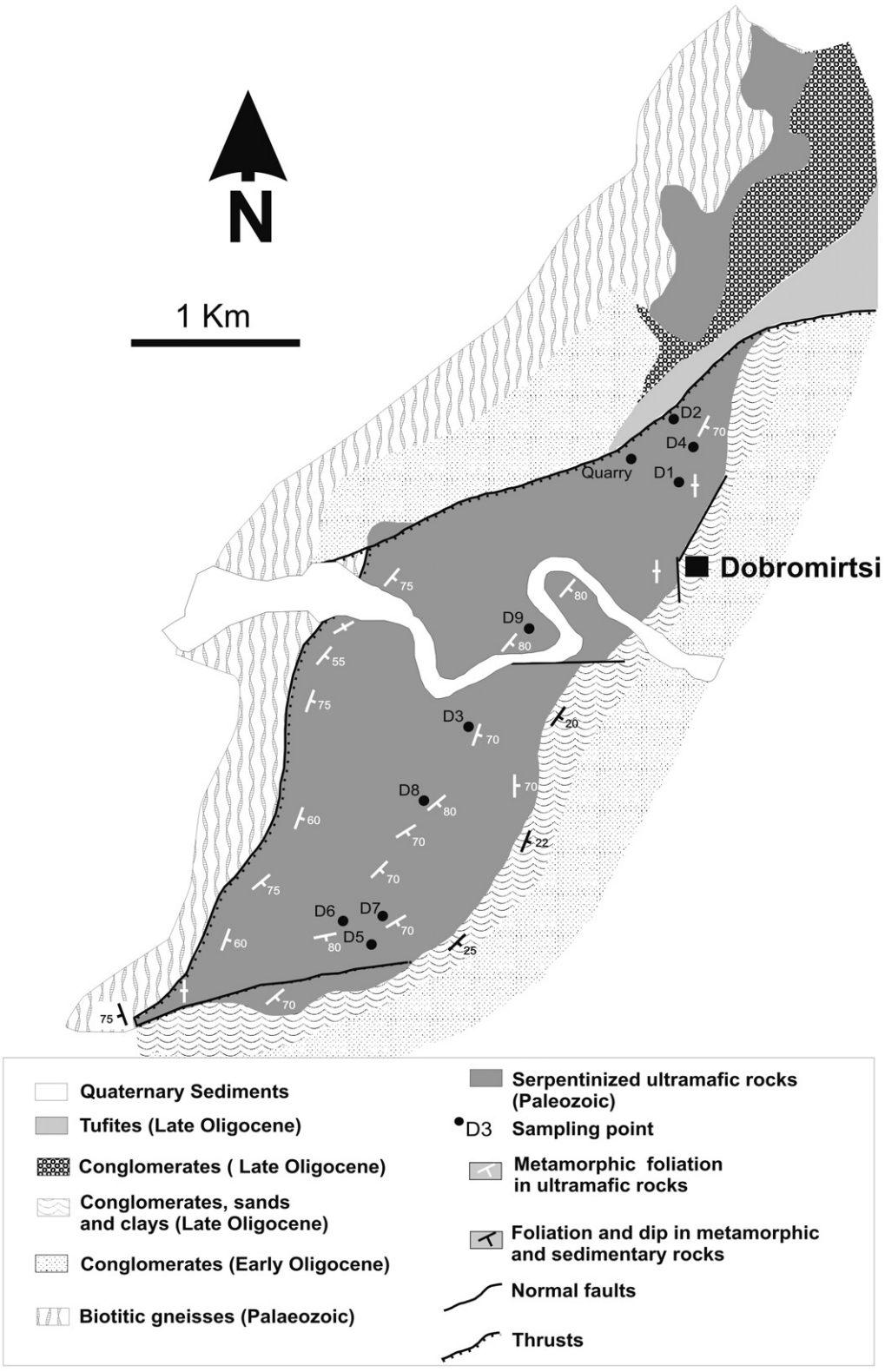

FIGURE 2 | **Simplified geological map of the Dobromirtsi Ultramafic Massif (modified from Payakov et al., 1961).**

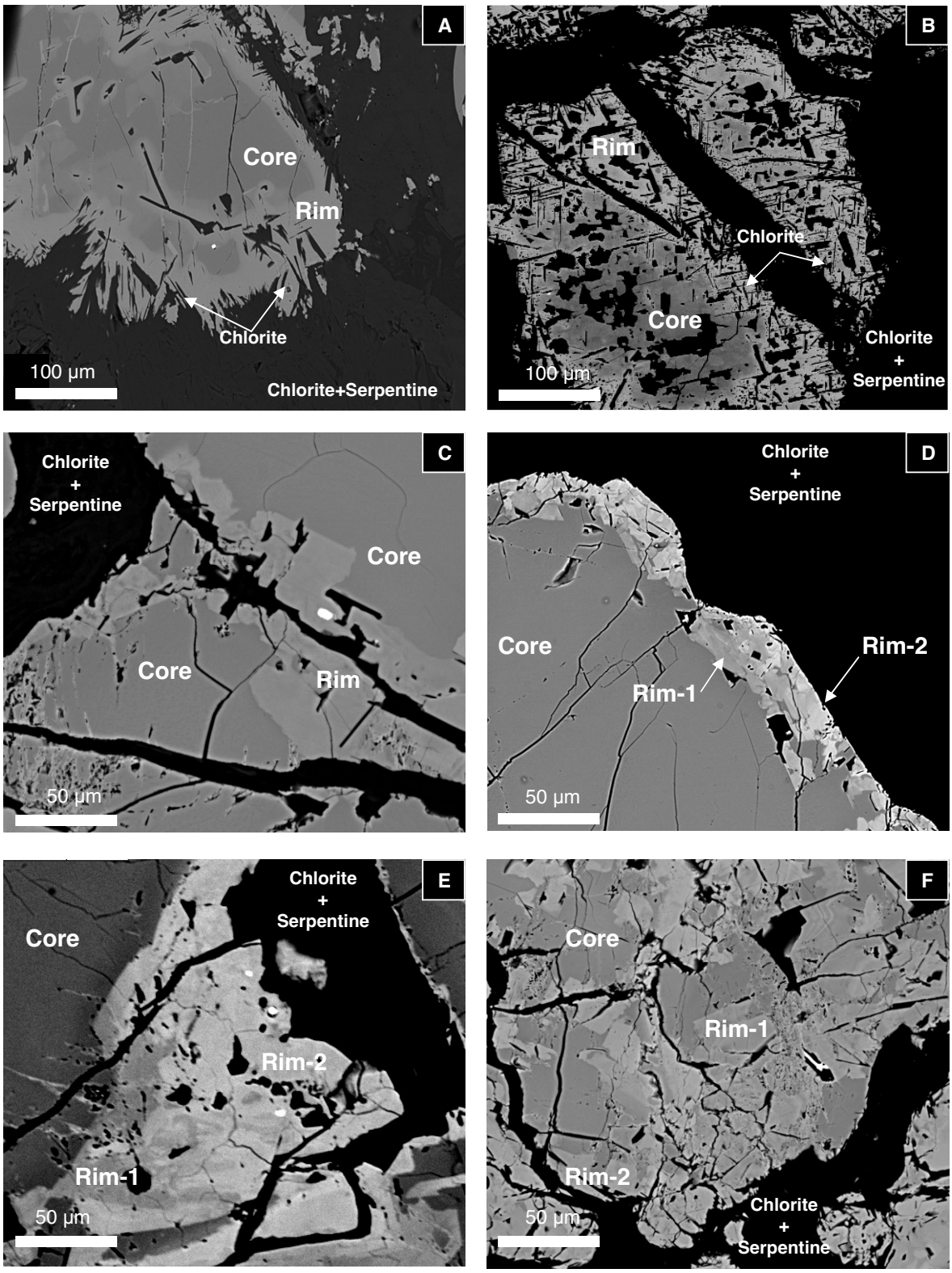

FIGURE 3 | **Back-scattered electron microphotographs illustrating typical zoning patterns of chromite ores from Dobromirtsi. A) concentrically zoned chromite crystal from D2 chromitite, showing a dark central zone (core) and an outer light-coloured zone (rim). Note that the rim contains abundant inclusions of chlorite. The white spot in the core is a minute inclusion of laurite (RuS_2). B) zoned chromite crystal of D2 chromitite. Note that the altered margin host very abundant inclusions of chlorite. C) zoned chromite crystal from D6 chromitite, showing alteration advancing from margins and open fractures inwards. D) zoned chromite crystal of D1 chromitite showing an altered margin made up of two optically and chemically differentiated rims. E) detail of the previous grain showing the unaltered core and the two alteration rims. The white spots in Rim-2 correspond to inclusions of Ni-arsenides F) complex irregular zoning in chromite of D1 chromitite.**

Individual chromite crystals are often fractured. Most of them show irregular optical zoning (Figs. 3A-F). Zoning is usually concentric, advancing from rims and open fractures inwards (Fig. 3A-E), although irregular and complex patterns with patches of unaltered and/or altered zones are also present (Fig. 3F). Chromite from D1 and D9 ore bodies show rims with two optically different zones (Figs. 3E and F). Chromite cores characteristically have rounded shapes, separated from the altered rims by sharp contacts. The outermost altered zones often develop a porous texture containing abundant inclusions of secondary silicates such as serpentine or mostly chlorite (Fig. 3A and B).

The interstitial serpentine matrix of chromitites consists of mesh-textured lizardite partly replaced by antigorite, together with chlorite, talc and carbonates. Chlorite forms either intergrowth aggregates with serpentine or aureoles that surround chromite; in the latter case, composition approaches chromium clinochlore. Talc forms after pyroxenes, whilst carbonates occur as tiny (less than 1cm thick) cross-cutting veins in chromite and serpentinite matrix. Traces of magnetite and brucite also occur in the serpentine matrix.

Mineral Chemistry

Although most chromite grains of the studied chromitites show systematic core to rim, or irregular compositional variations, those from the massive-textured ores of the D3, D4 and D8 do not show any compositional variation. The composition of these chromites clearly plots within the field of podiform (ophiolite) chromitites (Fig. 4) having Cr# from 0.55 to 0.77, and Mg# from 0.53 to 0.69. Whereas Mg# of chromite is very similar in the three ore bodies, Cr# increases from D8 to D4 and to D3. Similar compositions are preserved in the cores of chromite from D1 and D5 ore bodies (Fig. 4). Chromite cores from D1 chromitite show variable Cr# (from 0.57 to 0.71) and the highest Mg# (up to 0.78). In contrast, those from D5 chromitite have similar Mg# (from 0.51 to 0.67) like the unaltered chromite, but the lowest Cr# (from 0.53 to 0.57). Chromite from the latter chromitite show core to rim compositional variations (Fig. 4) characterized by strong Cr_2O_3 and FeO enrichment (Cr# varies from 0.53 to 0.85, and Mg# from 0.85 to 0.18) with no increase in Fe_2O_3 (Fig. 5). Cores of D2 chromitite are very heterogeneous showing significant Cr# and Mg# variations (from 0.60 to 0.74 and from 0.31 to 0.38, respectively) (Fig. 4). These compositions overlap those of the chromite rims of D5 chromitites (Fig. 4).

Core to rim, Fe^{3+}# variations in chromite are mainly observed in semi-massive- and disseminated-textured ores of D1, D2, D6 and D9 chromitites (Fig. 5). This figure shows the absence of Fe^{3+} enrichment in chromite from D3, D4, D8 and D5 chromite, as well as different trends of Fe^{3+} enrichment, compared to chromite from the other ore bodies studied. Core to rim, Fe^{3+} enrichment in D2 chromitite (Fe^{3+}# varies from 0.03 to 0.12) is accompanied by a slight increase in FeO (Mg# varies from 0.38 to 0.17) (Fig. 5) and a strong Cr_2O_3 enrichment (Cr# varies from 0.81 to 0.94) (Fig. 6). In contrast, in D6 chromitite, Fe^{3+} enrichment from core to rim (Fe^{3+}# varies from 0.06 to 0.28) takes place without any variation in either FeO or Cr_2O_3 contents, but is associated with a strong loss of Al_2O_3 (Figs. 5 and 6). Chromite from D1 and D9 chromitites shows a more complex pat-

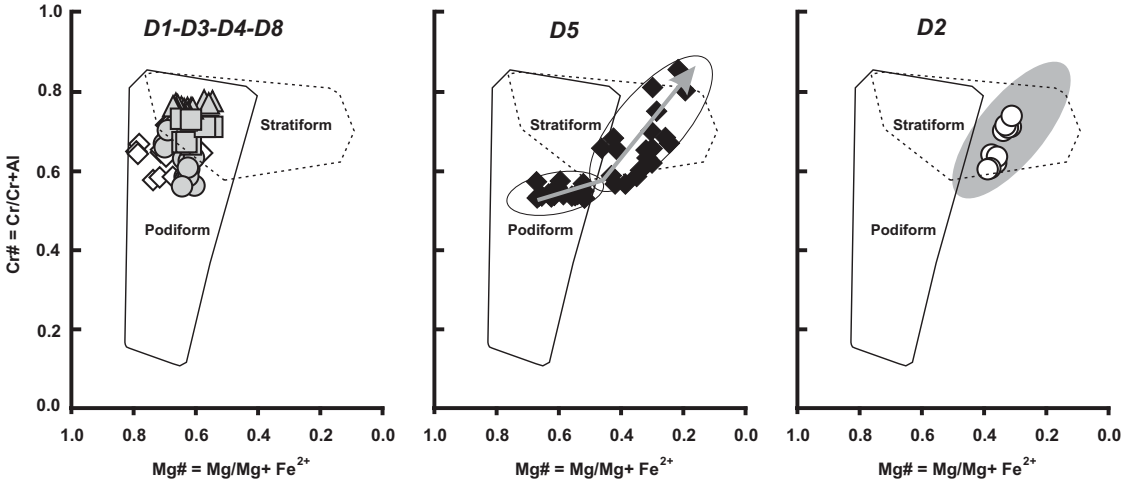

FIGURE 4 | **Plot of the composition of cromite with less than 5 wt.% Fe_2O_3 on the Cr# [Cr/Cr+Al] versus Mg# [Mg/Mg+Fe] diagram. Compositional fields of podiform and stratiform chromitites are from Leblanc and Nicolas (1992) and Irvine (1967), respectively. D1) white diamonds; D2) white circles; D3) grey triangles; D4) grey squares; D5) black diamonds; D8) grey circles. Arrows show the compositional variation, from core to rim, of zoned chromite from D5 chromitite. Grey field in D2 chromitite represents the compositional field of chromite rims of D5 chromitite.**

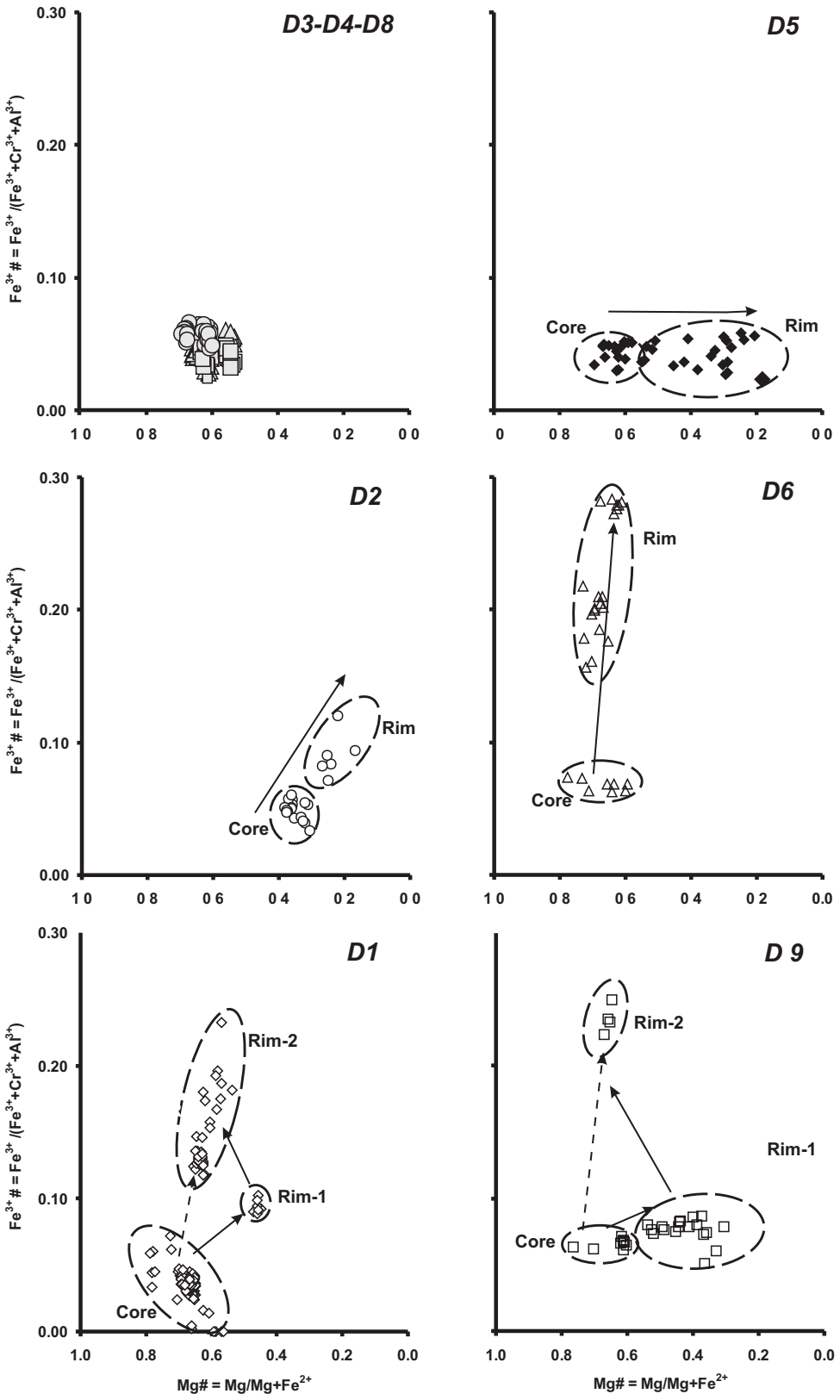

FIGURE 5 | **Compositional variations of chromite from the studied chromitites in terms of Fe^{3+}#= [Fe^{3+}/(Fe^{3+}+$Cr^{3+}$$Al^{3+}$)] and Mg# [Mg/Mg+$Fe^{2+}$)]. D1) white diamonds; D2) white circles; D3) grey triangles; D4) grey squares; D5) black diamonds; D6) white triangles; D8) grey circles; D9) white squares. Arrows show compositional variation from core to rims. Dashed arrows suggest that, locally, Rim-2 could develop directly from the unaltered core.**

tern of zoning with two alteration zones (Rim-1 and Rim-2) irregularly surrounding the unmodified or slightly modified cores (Figs. 3D-F and 5). The composition of chromite cores in D1 chromitite plots in an elongated field which suggest a compositional trend characterized by a slight increase in Fe_2O_3 (Fe^{3+}# varies from 0 to 0.08) and a significant depletion in FeO (Mg# varies from 0.56 to 0.79) (Fig. 5). Rim-1 forms around these cores by a slight increase in Fe_2O_3 (Fe^{3+}# varies from 0.09 to 0.10), a significant increase of FeO (Mg# varies from 0.47 to 0.45) and loss of Al_2O_3 (Cr# increases from 0.71 to 0.77) content (Figs. 4 and 5). Rim-2 (not always present) forms around Rim-1 (compositional trend drawn with a solid arrow in Fig. 5) or occasionally around cores (compositional trend drawn with a dashed arrow in Fig. 5) (Figs. 3D-F). The formation of this rim implies a further increase in Fe_2O_3 (Fe^{3+}# up to 0.23) coupled with a decrease in FeO (Mg# varies from 0.78 to 0.46) and a very significant decrease in Al_2O_3 content (Cr# varies from 0.64 to 0.91). The alteration trends identified in the different zones, observed in chromite from D9 chromitite are almost the same as those described in D1, except for the fact that the cores are more homogenous, having Fe_2O_3 contents that overlap the Fe_2O_3-richest zone of the field defined by the cores of D1 chromite (Fig. 5). Some of these trends are well illustrated in the profiles shown in Fig. 7 and representative analytical data are listed in tables 1 to 4.

DISCUSSION

Chromite from chromitites of the Dobromirtsi Ultramafic Massif is variably altered. The degree of alteration mainly depends on the chromite/silicate ratio and, to a lesser extent, on the size of chromitite bodies (large bodies tend to be massive). Thus, whereas chromite from D3, D4 and D8 ore bodies remains unaltered, chromite from the other ore bodies studied is affected by variable alteration degrees, showing different zoning patterns.

The alteration rim of chromite from D5 chromitite, as well as chromite cores of D2 chromitite, have a chemical composition that provides evidence of an alteration event characterized by FeO enrichment and Cr# increase

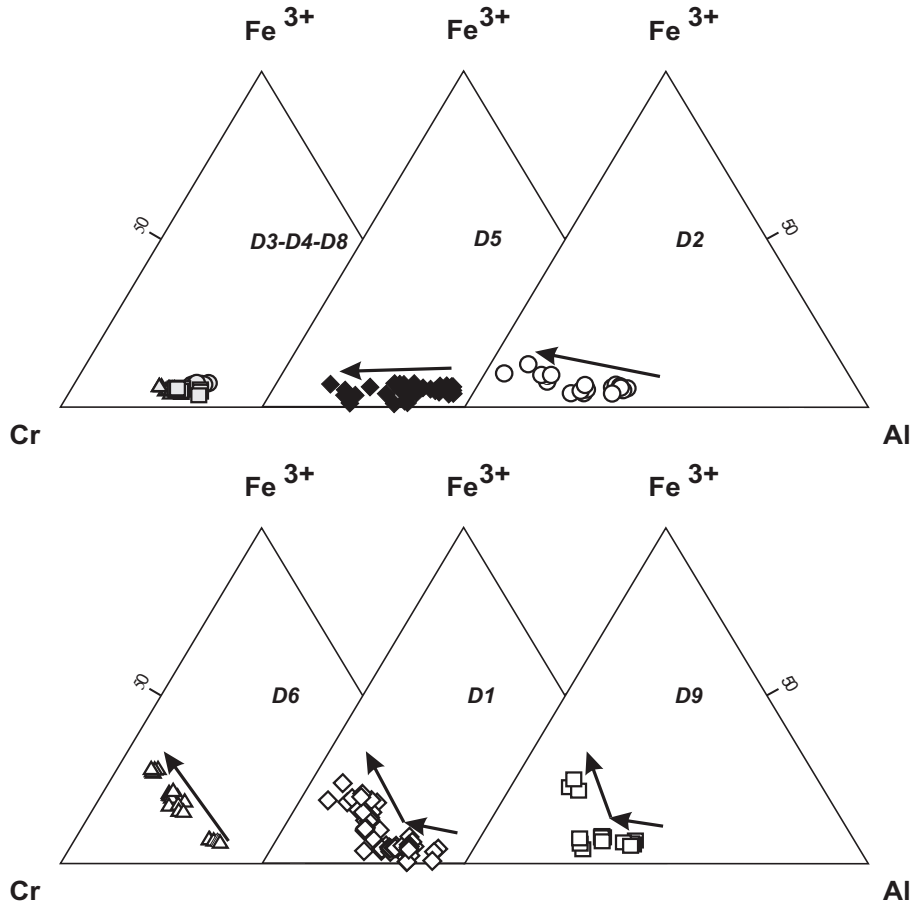

FIGURE 6 | **Compositional variation in chromite from the studied chromitites in terms of its Fe^{3+}, Cr^{3+} and Al^{3+} contents.**

(caused by loss of Al_2O_3) with little or no variation in Fe_2O_3 content (Fig. 6). According to Purvis et al. (1972), Evans and Frost (1975) and Suita and Streider (1996), such chemical variation is typical of chromite altered under greenschist facies metamorphism (Fig. 8). The origin of Fe^{2+}-, Cr^{3+}-enriched and Al-, Mg-depleted chromite can be explained using the modified reaction proposed by Kimball (1990). According to this author, at relatively high temperatures (> 400ºC) the Mg- and Al-rich component of the primary chromite reacts with MgO- and SiO_2-rich fluids to produce chlorite:

(I) $(Mg, Fe)(Al,Cr)_2O_4 + Fluid \rightarrow$
Chromite
$Mg_5AlSi_3O_{10}(OH)_8 + (Fe,Mg)(Cr,Al)_2O_4$
Chlorite

The formation of chlorite through this reaction implies outward diffusion of Al and Mg from chromite, leaving a residual Fe^{2+}-, Cr^{3+}-enriched and Al-, Mg-depleted chromite. The temperatures proposed by Kimball (1990) do not concur with those at which greenschist facies metamorphism takes places (200-400 ºC; Ernst, 1993). However, the combined serpentinization of olivine and pyroxene (Bach et al., 2006) at lower temperatures (200-300 ºC) could favour the creation of a MgO-, SiO_2-rich environment necessary for the Kimball reaction to take place.

The alteration rim surrounding chromite cores of D2 chromitite, as well as the inner alteration rim (Rim-1) surrounding the slightly altered chromite cores of D1 and D9 chromitites display a chemical composition, similar to that described in the alteration rim of chromite of D5 chromitite and the chromite cores of D2 chromitite in terms of FeO, MgO, Cr_2O_3 and Al_2O_3, but showing slight Fe_2O_3 enrichment (Figs. 5 and 6). These compositions also plot in the field of greenschist facies metamorphism (Fig. 8). Nevertheless, the slight Fe^{3+} enrichment in chromite suggests the beginning of a change in the alteration conditions to more oxidative states. According to Mellini et al. (2005), relatively high oxidative conditions favour the reaction of spinel (or the spinel component of chromite) with serpentine to produce chlorite and a Fe-rich, Cr-spinel intermediate between chromite and magnetite:

(II) $MgAl_2O_4 + 1.5Mg_3Si_2O_5(OH)_4 + H_2O + 0.083O_2 \rightarrow$
Al-Spinel Serpentine
$Mg_5AlSi_3O_{10}(OH)_8 + 0.167(Fe,Cr)_3O_4$
Chlorite Ferritchromite

Textural evidence and the observed chemical variations show that this Fe-rich, Cr-spinel occurs as an alteration rim of the previously altered chromite from D2 and as Rim-1 of chromites from D1 and D9 chromitites, formed by the reaction of the pre-existing chromite (unaltered or affected by the described early stages of greenschist facies metamorphism) with the serpentine of the silicate matrix. The

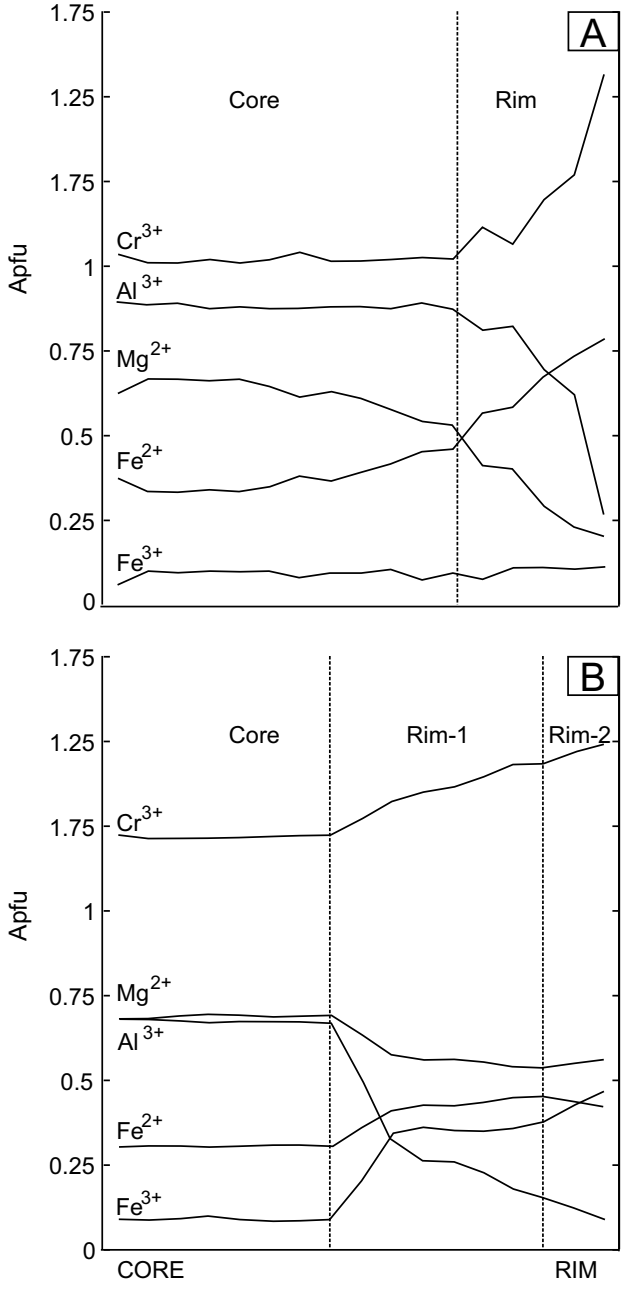

FIGURE 7 **Compositional variations of Cr^{3+}, Al^{3+}, Fe^{3+}, Fe^{2+} and Mg^{2+}, through representative zoned chromite grains showing the alteration zones identified in the studied chromites. Variations as determined by electron microprobe are shown in atoms per formula unit (*apfu*). A) zoned chromite grain of D5 chromitite illustrating core to rim, Fe^{2+} and Cr^{3+} enrichment and Mg^{2+} and Al^{3+} loss. B) zoned chromite from D1 chromitite showing an unaltered core and altered margin made up of two alteration rims. Rim-1 is characterized by Cr^{3+}, Fe^{3+} and Fe^{2+} increase and loss of Al^{3+} and Mg^{2+}, and Rim-2 is characterized by Fe^{3+} increase coupled with a decrease in Fe^{2+} and with opposite variations in Cr^{3+} and Al^{3+} contents.**

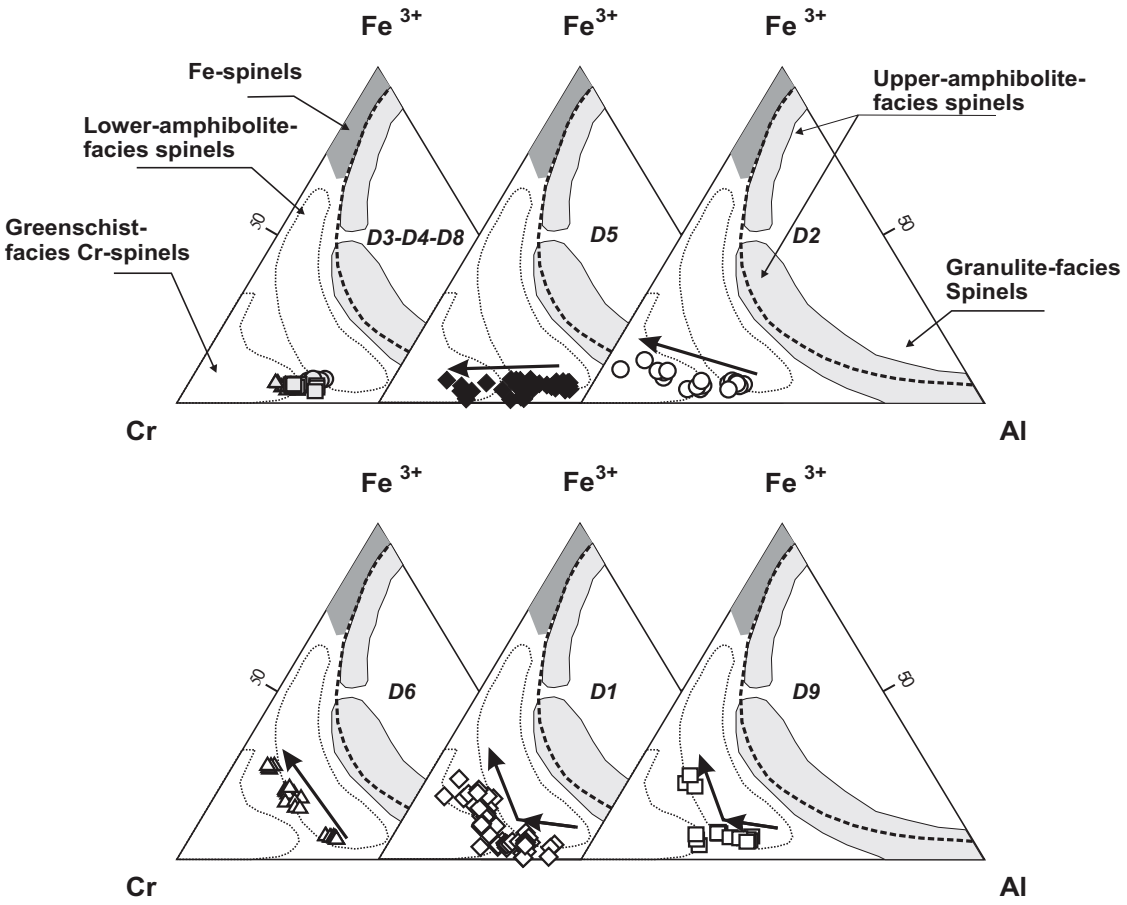

FIGURE 8 | **Compositional changes in chromites from Dobromirtsi expressed in a triangular Cr-Fe^{3+}-Al^{3+} plot with reference to the fields of the different metamorphic facies defined for Cr-spinels by Purvis et al., (1972); Evans and Frost, (1975), and Suita and Streider, (1996). D1) white diamonds; D2) white circles; D3) grey triangles; D4) grey squares; D5) black diamonds; D6) white triangles; D8) grey circles; D9) white squares. Arrows indicate the main compositional trends.**

lack of evidence of alteration in chromite from D1 and D9 chromitites during the early stages of greenschist facies metamorphism, shows either that it was not affected by this metamorphic event or, most probably, that it was completely obliterated by the subsequent oxidizing event. The $f(O_2)$ increase required for the formation of Fe-rich Cr-spinel might be associated with late stages of serpentinization during advanced steps of greenschist metamorphism, when olivine was totally replaced by serpentine (Eckstrand, 1975; Frost, 1985; Bach et al., 2006).

The composition of chromite from D6 chromitites, as well as Rim-2 of chromite from D1 and D9 shows the highest Fe^{3+} contents among the studied chromite. These compositions are typical for an Fe^{3+}-rich, Cr-spinel known in the literature as "ferritchromite" (Spangenber, 1943; Evans and Frost, 1975). In the studied chromitites, the formation of ferritchromite implies an alteration event characterized by a strong increase in Fe^{3+} associated with a strong loss of Al_2O_3 with little or no Cr_2O_3 and FeO variation. According to Fig. 8, this alteration event should have taken place during lower-temperature amphibolite facies metamorphism. Progressive Fe^{3+} increase relative to earlier altered chromites suggests an increase of the oxidative state with increasing metamorphism. Prograde metamorphism stopped serpentinization of pyroxene and olivine (Frost, 1985; Bach et al., 2006), favouring an oxidizing environment. As noted above, reaction II is mainly controlled by $f(O_2)$ in the environment. The progressive increase of $f(O_2)$ favoured the reaction of higher amounts of serpentine and chromite, producing chlorite (now found as inclusions at ferritchromite alteration margins or forming haloes around chromite) and ferritchromite. The shape of the contacts between ferritchromite rims and alteration Rim-1 or unaltered or slightly altered cores of chromite from D1, D9 and D6 chromitites (Fig. 3E) suggests that oxidizing fluids involved in the alteration process were very aggressive and also able to dissolve chromite, giving rise to a migration of Fe^{3+}, Al^{3+} and

Cr^{3+} out of chromite (Wylie et al., 1987). The decrease in FeO observed in the alteration Rim-2 of chromite of D1 chromitites (Figs. 5, 6 and 7) also suggests that the dissolution of chromite might favour the liberation of some amounts of Fe^{2+}, which was later oxidized to Fe^{3+}, therefore contributing to the increase in the amount of Fe^{3+} available for the formation of ferritchromite.

The local presence of some amounts of talc, brucite and carbonates, suggests that late, highly oxidizing conditions were accompanied by limited influence of CO_2-rich fluids (Eckstrand, 1975):

(III) $15Mg_3Si_2O_5(OH)_4 + 2Fe_3O_4 + 30CO_2 \rightarrow$
Serpentine Magnetite
$9Mg_3Si_4O_{10}(OH)_2 + 30(Mg_{0.9}\,Fe_{0.1})CO_3 + 27H_2O + ½\,O_2$
Talc Magnesite

The scarce proportion of these minerals in the studied chromitites allows us to deduce that their formation was a very late process, limited by the small amount of magnetite, generated when olivine was transformed to lizardite, during ocean-floor metamorphism. On the other hand, the preservation of chlorite/antigorite intergrowths in the altered silicate matrix between chromite grains, together with the absence of newly formed olivine (that forms after antigorite by dehydration at 500 ºC; Caruso and Chernosky, 1979) again suggest that the temperature did not exceed the range of lower amphibolite facies metamorphism.

The described evolution of the alteration process is summarized in Fig. 9. This simplified diagram shows that alteration rims in metamorphosed chromitites are a faithful record of the metamorphic path. As shown in Fig.8, low temperature serpentinization, occurring during ocean-floor metamorphism most probably did not produce any change in chromite composition as it took place under highly reducing conditions (Bach et al., 2006). However, with the increasing temperature, during the earlier stages of greenschist facies metamorphism, chromite reacts with Mg- and SiO_2-rich fluids losing Al^{3+} and Mg^{2+}, and giving rise to a new chromite rich in FeO and Cr_2O_3 in equilibrium with chlorite. A further increase in the metamorphic degree stops the serpentinization of olivine and pyroxene, promoting the creation of a relatively more oxidizing environment. Then, the reaction of the pre-existing chromite (both altered and unaltered) with serpentine results in the formation of a new alteration rim characterized by higher Fe^{3+} content. Under lower-temperature amphibolite facies conditions, chemical changes in chromite are characterized by a strong increase in the Fe_2O_3 content, demonstrating a significant increase of O_2. Under these oxidizing conditions, higher amounts of serpentine react with chromite, producing ferritchromite and an abundance of chlorite. At the end of the evolutionary history of these chromitites, serpentine reacted with brucite to form chlorite/antigorite intergrowths or with magnetite to form talc and carbonates (magnesite) in the silicate matrix of chromite or along late narrow veins.

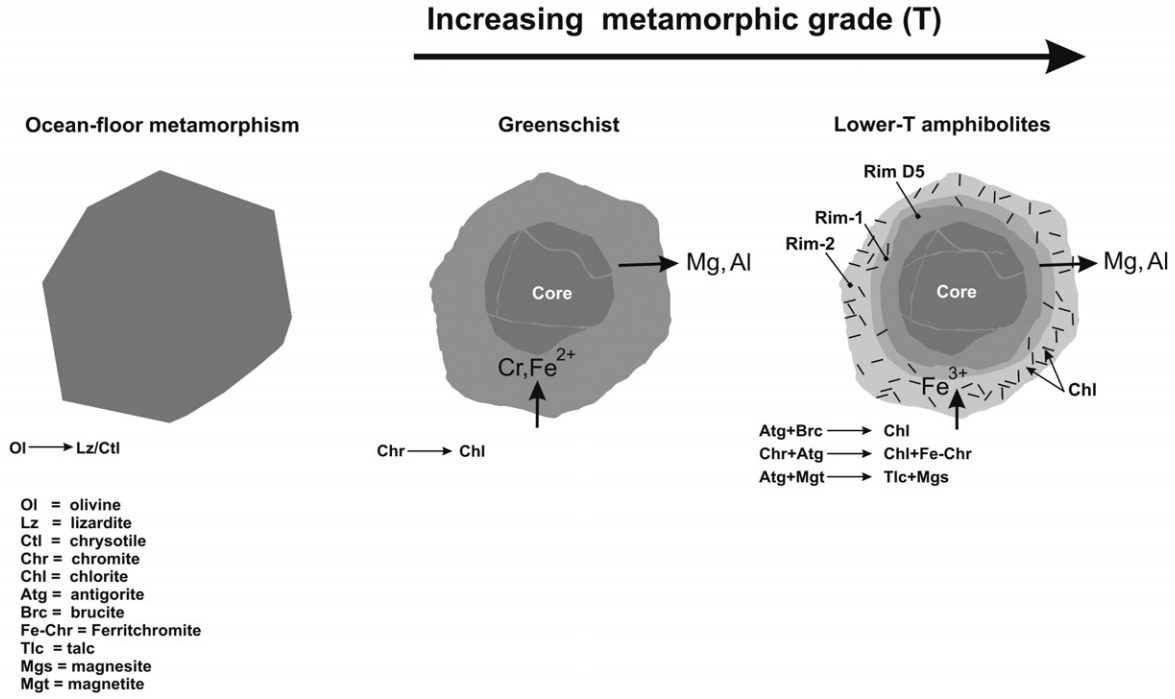

FIGURE 9 | **Schematic illustration of chemical changes in chromite during prograde alteration and metamorphism.**

CONCLUDING REMARKS

The study of chromitite samples from the nine chromite ore bodies of the Dobromirtsi Ultramafic Massif indicates that the chemical variation observed in the altered chromite, relative to primary chromite, reflects the effect of metamorphic reactions between chromite and the surrounding silicate matrix.

The detailed petrography and chemical investigation of chromitites indicates that alteration is very heterogeneous. The degree of alteration depends on the chromite/silicate ratio and, to a lesser extent on the size of the chromitite bodies. Thus, in massive-textured and big ore bodies chromite survives, showing very little or no alteration; in contrast, chromite from small ore bodies, usually with disseminated texture, is easily altered.

Alteration is recorded in individual chromite grains as irregular to concentric zones. Thus, three main alteration events have been identified. During the first one, lizardite replaced olivine and chromite remained unaltered. During the second event, the Mg- and Al-rich component of primary chromite reacted with MgO- and SiO_2-rich fluids to form chlorite, and chromite enriched in FeO and Cr_2O_3 and impoverished in Al_2O_3, with little or no variation in the Fe_2O_3 content. Finally, during the third event, unaltered or previously altered chromite reacted with already formed serpentine under oxidizing conditions to form new amounts of chlorite. As a result of this process, chromite strongly enriches in Fe^{3+} forming ferritchromite.

These alteration events characterize different steps of the prograde metamorphism that affected chromitites in accordance with the evolution of the regional metamorphism of central Rhodopes. The first one took place during ocean-floor metamorphism, whereas the second and third events occurred during greenschist and lower temperature amphibolite facies metamorphism, respectively.

ACKNOWLEDGEMENTS

We are indebted to K.S. Periov, local chief geologist for his help and attention during field work in the area and A. Rueda Torres (Department of Mineralogy and Petrology, University of Granada) for the preparation of the polished sections. We also acknowledge the assistance of X. Llovet (Serveis Cientificotècnics of the University of Barcelona), I. Sánchez Almazo (Centro Andaluz de Medio Ambiente of the Junta Andalucía-University of Granada), A. González Segura (Centro de Instrumentación Científica of the University of Granada) for their assistance with EPMA, ESEM and FESEM, respectively. The authors are also grateful to Drs. M. Mellini and N. Angeli for their constructive criticisms which greatly improved this manuscript. Likewise, we acknowledge Daniel Cooper for his help with the English language and A. Jabaloy for his help with the comprehension of the Geology of Rhodopes. This research was financially supported by the Spanish project CGL2007-61205 of the MEC, the CSIC-BAS collaborative project 2007BG0006, the research group (RNM 131) of the Junta de Andalucía, and an F.P.I grant BES-2005-8328 of the Spanish Ministry of Education and Sciences. Cynthia Voelker is acknowledged for her final review of the English writing.

REFERENCES

Arai, S., 1992. Chemistry of chromian spinel in volcanic rocks as a potential guide to magma chemistry. Mineralogical Magazine, 56, 173-784.

Bach, W., Paulick, H., Garrido, C.J., Ildefonse, B., Meurer, W., Humphris, S.E., 2006. Unravelling the sequence of serpentinization reactions: petrography, mineral chemistry, and petrophysics of serpentinites from MAR 15ºN (ODP Leg 209, Site 1274). Geophysical Research Letters, 25, 1467-1470.

Barnes, S.J., Roeder, P.L., 2001. The range of spinel compositions in terrestrial mafic and ultramafic rocks. Journal of Petrology, 42, 2279-2302.

Beeson, M.H., Jackson, E.D.,1969. Chemical composition of altered chromites from the Stillwater complex, Montana. American Mineralogist, 54, 1084-1100.

Bliss, N.W., MacLean, W.H., 1975. The paragenesis of zoned chromite from the Manitoba. Geochimica et Cosmochimica Acta, 39, 973-990.

Carmichael, I.S.E., 1967. The iron-titanium oxides of salic volcanic rocks and their associated ferromagnesian silicates. Contributions to Mineralogy and Petrology, 14, 36-64.

Caruso, LJ., Chernosky, J.V., 1979. The stability of lizardite. The Canadian Mineralogist, 17, 757-769.

Cerny, P., 1968. Comments on serpentinization and related metasomatism. American Mineralogist, 53, 1377-1385.

Dick, H.J.N., Bullen, T., 1984. Chromian spinel as a petrogenetic indicator in abysal and alpine-type peridotites and spatially associated lavas. Contributions to Mineralogy and Petrology, 86, 54-76.

Eckstrand, O.D., 1975. The Dumont serpentinite: a model for control of nickeliferous opaque mineral assemblages by alteration reactions in ultramafic rocks. Economic Geology, 70, 183-201.

Evans, B.W., Frost, B.R., 1975. Chrome-spinel in progressive metamorphism - a preliminary analysis. Geochimica et Cosmochimica Acta, 39, 959-972.

Frost, B.R., 1985. On the stability of sulfides, oxides and native metals in serpentinite. Journal of Petrology, 26, 31-63.

Garuti, G., Proenza, J.A., Zaccarini, F., 2007. Distribution and mineralogy of platinum-group elements in altered chromitites of the Campo Formoso layered intrusion (Bahia State,

Brazil): their control by magmatic and hydrothermal processes. Mineralogy and Petrology, 89, 159-188.

Hill, R., Roeder, P., 1974. The crystallization of spinel from basaltic liquid as a function of oxygen fugacity. Journal of Geology, 82, 709-729.

Irvine, T.N., 1967. Chromian spinel as a petrogenetic indicator; Part II, Petrologic applications. Canadian Journal of Earth Sciences, 4, 71-103.

Kimball, K.L., 1990. Effects of hydrothermal alteration on the composition of chromian spinels. Contributions to Mineralogy and Petrology, 105, 337-346.

Marchev, P., Kaiser-Rohrmeier, M., Heinrich C., Ovtcharova, M., Von Quadt, A., Raicheva, R., 2005. Hydrothermal ore deposits related to post-orogenic extensional magmatism and core complex formation: The Rhodope Massif of Bulgaria and Greece. Ore Geology Reviews, 27, 53-89.

Maurel, C., Maurel, P., 1982. Étude expérimentale de la distribution de l'aluminium entre bain silicaté basique et spinelle chromifère. Implications pétrogénétiques: teneur en chrome des spinelles. Bulletin de Minéralogie, 105, 197-202.

Mellini, M., Rumori, C., Viti, C., 2005. Hydrothermally reset magmatic spinels in retrograde serpentinites: formation of "ferritchromit" rims and chlorite aureoles. Contribution to Mineralogy and Petrology, 149, 266-275.

Leblanc, M., Nicolas, A., 1992. Les chromitites ophiolitiques. Chronique de la Recherche Minière, 507, 3-25.

Payakov, I., Zhelyaskova-Panayotova, M., Ivehinova, L., 1961. Structural-textural peculiarities and mineral composition of chromite ore from from Dobrimirtzi deposit. Annuaire de l'Université de Sofia, 56, 219-229.

Prichard, H.M., Sá, J.H.S., Fisher, P.C., 2001. Platinum-group mineral assemblages and chromite composition in the altered and deformed Bacuni complex, Amapa, northeastern Brazil. The Canadian Mineralogist, 39, 377-396.

Proenza, J.A., Gervilla, F., Melgarejo, J.C., Bodinier, J.L., 1999. Al-rich and Cr-rich chromitites from the Mayarí-Baracoa ophiolitic belt (eastern Cuba): consequence of interaction between volatile-rich melts and peridotites in suprasubduction mantle. Economic Geology, 94, 547-566.

Proenza, J.A., Ortega-Gutiérrez, F., Camprubí, A., Tritlla, J., Elías-Herrera, M., Reyes-Salas, M., 2004. Paleozoic serpentinite-enclosed chromitites from Tehuitzingo (Acatlán Complex, southern Mexico): a petrological and mineralogical study. Journal of South American Earth Sciences, 16, 649-666.

Proenza, J.A., Zaccarini, F., Escayola, M., Cábana, C., Shalamuk, A., Garuti, G., 2008. Composition and textures of chromite and platinum-group minerals in chromitites of the western ophiolitic belt from Córdoba Pampeans Ranges, Argentine. Ore Geology Reviews, 33, 32-48.

Purvis, A.C., Nesbitt, R.W., Halberg, J.A., 1972. The geology of part of Carr Boyd Complex and its associated nickel mineralization, Western Australia. Economic Geology, 67, 1093-1113.

Roeder, P.L., Reynolds, I., 1991. Crystallization of chromite and chromium solubility in basaltic melts. Journal of Petrology, 32, 909-934.

Spangenberg, K., 1943. Die Chromerzlagerstätte von Tampadel Zobten. Zeitschrift für praktische Geologie, 51, 13-35.

Stowe, C.W., 1994. Compositions and tectonic setting of chromite deposits through time. Economic Geology, 89, 528-564.

Suita, M.T., Streider, A.J., 1996. Cr-spinels from Brazilian mafic-ultramafic complexes: metamorphic modifications. International Geology Review, 38, 245-267.

Thalhammer, O.A.R., Prochaska, W., Mühlhans H.W., 1990. Solid inclusions in chrome-spinels and platinum group element concentrations from the Hochgrössen and Kraubath ultramafic massif (Austria). Contributions to Mineralogy and Petrology, 105, 66-80.

Thayer T.P., 1966. Serpentinisation considered as a constant volume metasomatic process. American Mineralogist, 51, 685-710.

Ulmer, G.C., 1974. Alteration of Chromite during Serpentinization in the Pennsylvania-Maryland District. American Mineralogist, 59, 1236-1241.

Wylie, A.G., Candela, P.A., Burke, T.M., 1987. Compositional zoning in unusual Zn-rich chromite from Sykesville district of Maryland and its bearing on the origin of "ferrichromit". American Mineralogist, 72, 413-422.

Zaccarini, F., Proenza, J.A., Ortega-Gutiérrez, F., Garuti., G., 2005. Platinum group minerals in ophiolitic chromitites from Tehuitzingo (Acatlán complex, southern Mexico): implications for post-magmatic modification. Mineralogy and Petrology, 84(3-4),147-168.

Zhelyaskova-Panayotova, M., Economou-Eliopoulos, M., 1994. Platinum-group elements and gold concentration in oxide and sulfide mineralizations from ultramafic rocks of Bulgaria. Annuaire de l'Université de Sofia, 86(1), 196-218.

Zhelyaskova-Panayotova, M., Zinzov, Z., Pashov, 2000. Hydrothermal gold mineralization in ultrabasites near Dobromirtsi village, Kurdjali region. Annuaire de l'Université de Sofia, 93(1), 173-186.

Zhou, M.F., Robinson, P.T., 1997. Origin and tectonic environment of podiform chromite deposits. Economic Geology, 92, 259-262.

Zhou, M.F., Sun, M., Keays, R.R., Kerrich, R.W., 1998. Controls on platinum-group elemental distributions of podiform chromitites: A case study of high-Cr and high-Al chromitites from Chinese orogenic belts. Geochimica et Cosmochimica Acta, 62, 677-688.

Manuscript received May 2008;
revision accepted January 2009;
published Online September 2009.

APPENDIX

Analytical data

TABLE 1 | **Selected representative analyses of unaltered chromite.**

Sample/Point	d1-3	d1-6-1	d3-102	d3-104	d4-102	d4-101	d5-202	d5-202	d8-205	d8-209
SiO_2	0.12	0.07	0.21	0.25	0.11	0.18	0.02	0.01	0.02	0.05
TiO_2	0.3	0.25	0.21	0.24	0.25	0.24	0.2	0.23	0.38	0.37
Al_2O_3	16.76	18.88	12.59	12.91	15.23	17.28	24.81	24.57	17.79	21.79
Cr_2O_3	51.97	50.34	56.84	54.92	52.4	50.08	42.75	41.89	49.69	44.25
Fe_2O_3	3.51	3.64	3.89	3.51	3.52	3.42	2.58	4.23	4.86	4.96
FeO	12.63	11.96	12.71	14.23	16.6	14	14.58	13.01	12.14	14.78
MnO	0.5	0.54	0.56	0.56	0.65	0.5	0.4	0.39	0.38	0.35
MgO	14.23	14.95	13.94	12.75	11.39	13.26	13.62	14.61	14.83	13.56
ZnO	0.1	0.06	0.1	0.06	0.07	0	-	-	-	-
NiO	0.19	0.15	0.15	0.1	0.19	0.12	-	-	-	-
Total Ox%	100.3	100.84	101.21	99.53	100.42	99.08	98.96	98.94	100.1	100.11
Si	0	0	0.01	0.01	0	0.01	0	0	0	0
Ti	0.01	0.01	0.01	0.01	0.01	0.01	0	0.01	0.01	0.01
Al VI	0.62	0.68	0.47	0.49	0.57	0.64	0.89	0.88	0.65	0.78
Cr	1.28	1.22	1.42	1.4	1.32	1.25	1.04	1.01	1.22	1.07
Fe^{3+}	0.08	0.08	0.09	0.09	0.09	0.08	0.06	0.09	0.11	0.12
Fe^{2+}	0.33	0.31	0.34	0.38	0.44	0.37	0.37	0.33	0.32	0.38
Mn^{2+}	0.01	0.01	0.02	0.02	0.02	0.01	0.01	0.01	0.01	0.01
Mg	0.66	0.68	0.66	0.61	0.54	0.63	0.62	0.66	0.68	0.62
Zn	0	0	0	0	0	0	-	-	-	-
Ni	0.01	0	0	0	0.01	0	-	-	-	-
Cr#	0.68	0.64	0.75	0.74	0.7	0.66	0.54	0.53	0.65	0.58
Mg#	0.67	0.69	0.66	0.62	0.55	0.63	0.63	0.67	0.69	0.62
Fe#	0.33	0.31	0.34	0.38	0.45	0.37	0.37	0.33	0.32	0.38
Fe^{3+}#	0.04	0.04	0.05	0.04	0.04	0.04	0.03	0.05	0.06	0.06

TABLE 2 | **Selected representative analyses of FeO-enriched and Al_2O_3- and MgO- depleted chromite (rim of chromite from D5 chromitites and chromite cores of D2 chromitites).**

Sample/Point	d2B-1-1	d2B-1-2	d2B-1-3	d2B-1-4	d2B-1-5	d5-202-1	d5-202-2	d5-202-3	d5-202-4	d5-202-5
SiO_2	0.11	0.07	0.11	0.09	0.13	0.07	0.08	2.21	0.78	0.06
TiO_2	0.42	0.39	0.28	0.35	0.34	0.18	0.16	0.17	0.15	0.12
Al_2O_3	18.17	18.38	12.66	17.91	19.14	14.69	20.67	8.49	6.51	9.13
Cr_2O_3	44.36	44.83	53.3	45.84	45.36	47.32	44.09	54.11	56.72	55.95
Fe_2O_3	4.51	4.26	2.62	4.92	3.97	4.46	3.35	2.63	4.15	1.77
FeO	22.98	23.08	24.39	23.2	22.89	25.51	23.85	26.17	26.86	26.69
MnO	0.73	0.78	0.78	0.73	0.68	1.31	1.26	1.49	1.58	1.39
MgO	7.25	7.23	6.04	7.4	7.8	4.7	6.87	5.98	3.89	3.34
ZnO	0.12	0.07	0.07	0.13	0.11	-	-	-	-	-
NiO	0.08	0.12	0.05	0.12	0.05	-	-	-	-	-
Total Ox%	98.73	99.2	100.29	100.7	100.48	98.23	100.32	101.26	100.64	98.45
Si	0	0	0	0	0	0	0.01	0.07	0.03	0
Ti	0.01	0.01	0	0.01	0.01	0.01	0.01	0	0.04	0
Al VI	0.71	0.71	0.5	0.68	0.73	0.59	0.78	0.34	0.26	0.38
Cr	1.15	1.16	1.41	1.17	1.15	1.27	1.12	1.44	1.56	1.56
Fe^{3+}	0.11	0.11	0.06	0.12	0.09	0.12	0.08	0.06	0.11	0.05
Fe^{2+}	0.63	0.63	0.68	0.63	0.62	0.73	0.64	0.74	0.78	0.78
Mn^{2+}	0.02	0.02	0.02	0.02	0.02	0.04	0.03	0.04	0.04	0.04
Mg	0.35	0.35	0.3	0.35	0.37	0.23	0.33	0.3	0.2	0.17
Zn	0	0	0	0	0	-	-	-	-	-
Ni	0	0	0	0	0.001	-	-	-	-	-
Cr#	0.62	0.62	0.74	0.63	0.61	0.68	0.59	0.81	0.85	0.8
Mg#	0.36	0.36	0.31	0.36	0.38	0.25	0.34	0.29	0.21	0.18
Fe#	0.97	0.97	0.97	0.97	0.97	0.95	0.95	0.94	0.94	0.95
Fe^{3+}#	0.06	0.05	0.03	0.06	0.05	0.06	0.04	0.04	0.06	0.02

TABLE 3 | **Selected representative analyses of Fe_2O_3- and FeO-enriched, and Al_2O_3- and MgO- depleted chromite (rim of chromite from D2 and Rim-1 in D1 and D9 chromitites)**

Sample/Point	d1-3-1	d1-3-2	d1-3-4	d2B-1-6	d2B-1-7	d2B-1-8	d2B-1-9	D9-202-1	D9-202-2	D9-202-3
SiO_2	0.19	0.13	0.11	0.16	0.11	0.27	0.92	0	0	0.24
TiO_2	0.31	0.36	0.35	0.45	0.44	0.8	1.35	0.41	0.36	0.36
Al_2O_3	10.2	10.35	10.2	7.54	8.26	8.08	2.32	15.44	15.12	14.69
Cr_2O_3	50.65	50.7	50.49	53.53	53.86	53.49	53.31	49.11	47.92	47.07
Fe_2O_3	7.9	7.02	7.55	6.2	5.32	6.13	6.18	6.01	6.34	6.89
FeO	18.83	18.59	18.56	25.39	25.25	25.45	27.59	17.78	21.18	22.65
MnO	0.55	0.61	0.61	0.93	0.87	0.87	0.8	0.38	0.78	0.68
MgO	8.94	8.83	8.83	4.55	4.75	5.21	3.09	10.87	8.32	7.63
ZnO	0.08	0.08	0.12	0.14	0.08	0.08	0.11	-	-	-
NiO	0.33	0.35	0.33	0.06	0.04	0.13	0.24	-	-	-
Total Ox%	97.96	97.01	97.14	98.96	98.98	100.49	95.91	100	100.02	100.19
Si	0.01	0	0	0.01	0	0.01	0.04	0	0	0.01
Ti	0.01	0.01	0.01	0.01	0.01	0.02	0.04	0.01	0.01	0.01
Al VI	0.41	0.42	0.41	0.31	0.34	0.33	0.1	0.59	0.58	0.57
Cr	1.36	1.37	1.37	1.49	1.49	1.45	1.58	1.25	1.24	1.23
Fe^{3+}	0.2	0.18	0.2	0.16	0.14	0.16	0.17	0.15	0.16	0.17
Fe^{2+}	0.54	0.53	0.53	0.75	0.74	0.73	0.86	0.48	0.58	0.62
Mn^{2+}	0.02	0.02	0.02	0.03	0.03	0.03	0.03	0.01	0.02	0.02
Mg	0.45	0.45	0.45	0.24	0.25	0.27	0.17	0.52	0.41	0.37
Zn	0	0	0	0	0	0	0	-	-	-
Ni	0.01	0.01	0.01	0	0	0	0.01	-	-	-
Cr#	0.77	0.77	0.77	0.83	0.81	0.82	0.94	0.68	0.68	0.68
Mg#	0.46	0.46	0.46	0.24	0.25	0.27	0.17	0.52	0.41	0.37
Fe#	0.54	0.54	0.54	0.76	0.75	0.73	0.83	0.48	0.59	0.63
Fe^{3+}#	0.1	0.09	0.1	0.08	0.07	0.08	0.09	0.07	0.08	0.09

TABLE 4 | **Selected representative analyses of ferritchromite (rim of chromite from D6 and Rim-2 in chromite from D1 and D9 chromitites).**

Sample/Point	d1-6-2	d1-6-3	d1-6-4	d6-206-1	d6-206-2	d6-206-3	d6-206-4	D9-202-4	D9-202-5	D9-202-6
SiO_2	0.13	0.2	0.1	2.9	0.07	0.02	0.99	0.03	0.06	0.02
TiO_2	0.45	0.41	0.4	0.27	0.3	0.52	0.48	0.44	0.38	0.4
Al_2O_3	4.16	3.59	6.24	10.15	8.98	4.55	5.28	7.02	7.46	6.99
Cr_2O_3	49.54	53.21	50.88	44.47	47.68	46.35	45.77	45.63	46.14	47.53
Fe_2O_3	17.73	13.67	13.44	13.59	17.04	21.84	22.09	19.65	18.5	18.52
FeO	14.69	15.71	14.75	11.26	11.62	13.65	12.24	12.55	12.17	12.47
MnO	0.64	0.65	0.57	0.58	0.54	0.68	0.73	0.58	0.59	0.67
MgO	10.92	10.24	11.02	16.75	14.08	12.12	14.34	12.94	13.15	13.1
ZnO	0.04	0.04	0.06	-	-	-	-	-	-	-
NiO	0.61	0.41	0.43	-	-	-	-	-	-	-
Sum Ox%	98.9	98.13	97.89	99.97	100.31	99.72	101.92	98.85	98.45	99.7
Si	0	0.01	0	0.09	0	0	0.03			
Ti	0.01	0.01	0.01	0.01	0.01	0.01	0.01	0	0	0
Al VI	0.17	0.15	0.25	0.38	0.34	0.18	0.2	0.01	0.01	0.01
Cr	1.34	1.46	1.38	1.11	1.22	1.24	1.17	0.28	0.29	0.27
Fe^{3+}	0.46	0.36	0.35	0.32	0.42	0.55	0.54	1.21	1.22	1.24
Fe^{2+}	0.42	0.46	0.42	0.3	0.32	0.39	0.33	0.49	0.47	0.46
Mn^{2+}	0.02	0.02	0.02	0.02	0.02	0.02	0.02	0.35	0.34	0.35
Mg	0.56	0.53	0.56	0.79	0.68	0.61	0.69	0.02	0.02	0.02
Zn	0	0	0	-	-	-	-	0.65	0.66	0.65
Ni	0.02	0.01	0.01	-	-	-	-	-	-	-
								-	-	-
Cr#	0.89	0.91	0.85	0.75	0.78	0.87	0.85	0.96	0.97	0.96
Mg#	0.57	0.54	0.57	0.73	0.68	0.61	0.68	0.03	0.04	0.04
Fe#	0.43	0.46	0.43	0.27	0.32	0.39	0.32	0.97	0.96	0.96
Fe^{3+}#	0.23	0.18	0.18	0.18	0.21	0.28	0.28	0.81	0.8	0.81